Equation of State of Ethylene Vapor Between 223 and 273 K by the Burnett Method

J. M. H. Levelt Sengers[1] **and J. R. Hastings**[1,2]

Measurements are reported of the equation of state of ethylene in the vapor phase between 223 and 273 K by the Burnett method. (P, ρ, T) values are reported on six isotherms at 10 K intervals. Virial coefficients have been obtained in this range both for ethylene and for helium. The Burnett isotherms were coupled isochorically; this revealed a small but noticeable adsorption effect. Isochoric intersections with the phase boundary were performed to obtain values for the vapor pressure and the vapor density. Again, clear indications of surface effects were found. Our results have been compared with recent work by Douslin and Harrison, by Waxman and Davis, and by Thomas and Zander. The agreement with the work of Douslin and Harrison is striking: better than 2 parts in 10^4 in pressure and better than 1 cm^3 · mol^{-1} in the second virial coefficient. The agreement with the McCarty-Jacobsen formulation is somewhat less satisfactory. A discussion of the various factors determining the reliability of our results is given.

KEY WORDS: Burnett method; equation of state; ethylene; helium; saturation density; vapor phase; virial coefficients.

1. INTRODUCTION

Measurements of the equation of state of ethylene vapor are presented as part of a joint industry—U.S. Government project aimed at obtaining authoritative thermodynamic tables for this major chemical. Our work supplements and extends that of Douslin and Harrison [1]. Their lowest temperature was 238 K, while their pressures ranged from saturation down to 1.3 MPa. Our lowest temperature is 223 K, and our pressures range from saturation to 0.23 MPa. For a highly nonideal vapor, such as that of ethylene within 60 K of its

---

[1]Thermophysics Division, National Bureau of Standards, Washington, D.C. 20234, U.S.A.
[2]Presently in the Electrical Measurements and Standards Division, N.B.S., Washington, D.C.

critical point (282 K), it was considered important to include measurements at pressures as low as could have been measured accurately.

Our method, to be briefly described in Section 2, is the Burnett method; Burnett isotherms were measured at 10 K intervals from 273.15 K downward, both for helium and for ethylene. The helium results are reported in Section 3; they yield the volume ratio N and a set of helium second virials. The ethylene results were analyzed by a nonlinear regression method developed by Waxman et al. [2]. The results, tables of (P, ρ, T) for ethylene vapor, plus values of several virial coefficients are reported in Section 4 and compared with the data of Douslin and Harrison [1], Waxman and Davis [3], Thomas and Zander [4], and with the correlation of McCarty and Jacobsen [5]. The Burnett isotherms were coupled isochorically, as proposed by Pope et al. [6] and by Hall and Eubank [7]. This procedure permits a check on adsorption. A small but noticeable effect was found (Section 5).

The highest fill pressure of each Burnett run was chosen close to saturation. By lowering the temperature a few degrees, the two-phase region was entered isochorically. The sharp change in the slope of the (P, T) isochore locates the phase boundary. The results are compared with the data of Douslin and Harrison [1] (Section 6). Again, indications of adsorption effects were found. Section 7 contains concluding remarks regarding the reliability of the method and the accuracy of the results obtained.

2. APPARATUS, METHOD, SAMPLE

Our Burnett apparatus has been described in detail previously [8–10]. The two gold-plated stainless steel vessels, of approximately 10 cm^3 and 5 cm^3 volume, the pressure transducer, and the fill and expansion valves were all submerged in a thermostatic fluid that was temperature-controlled to better than 1 mK. The temperature was continuously monitored with a quartz thermometer, which was compared daily with an NBS-calibrated platinum thermometer to a precision of 0.2 mK. Pressures were measured on a controlled-clearance gas-lubricated piston gage [8, 9] that we estimate to have an accuracy of 5 parts in 10^5 in pressure. The barometric pressure was read to 3×10^{-6} MPa on an aneroid barometer that was intercompared with a master gage at NBS.

In the Burnett method, successive gas expansions are made from the principal vessel I into the evacuated second vessel II. After equilibration, the pressure is measured. Information on the nonideality of the gas is obtained by comparing the ratio of the pressure before and after expansion with the volume ratio of the vessels, $N = (V_{\mathrm{I}} + V_{\mathrm{II}})/V_{\mathrm{I}}$. The volume ratio is obtained from a series of expansions with helium; here the pressure ratios differ only slightly from the volume ratios and can therefore be safely extrapolated to

zero pressure to yield the volume ratio or cell constant N (Section 3). In the analysis of the Burnett runs of ethylene, the value of N obtained from the helium expansions was used.

For ethylene, two Burnett runs were taken along each isotherm. After completion of the two runs, the system was filled once more at the highest pressure in the second run. The temperature was then lowered by 10 K and a new Burnett isotherm measured. On these two isotherms, one thus obtains several pairs of points at the same density, save for minor corrections for pressure and temperature expansion of the vessels. Figure 1, which indicates the locations of the measured points in the (T, ρ) plane, shows, by vertical bars, the points that have thus been coupled isochorically. It also shows how small isochoric excursions from the highest pressure point on each isotherm bring the system into the two-phase region, which procedure permits measurement of the vapor pressure and the calculation of the vapor density.

Our sample was nominally 99.99% pure ethylene [9, 10]. Principal contaminants according to an analysis performed at NBS, were 83 ppm CH_4,
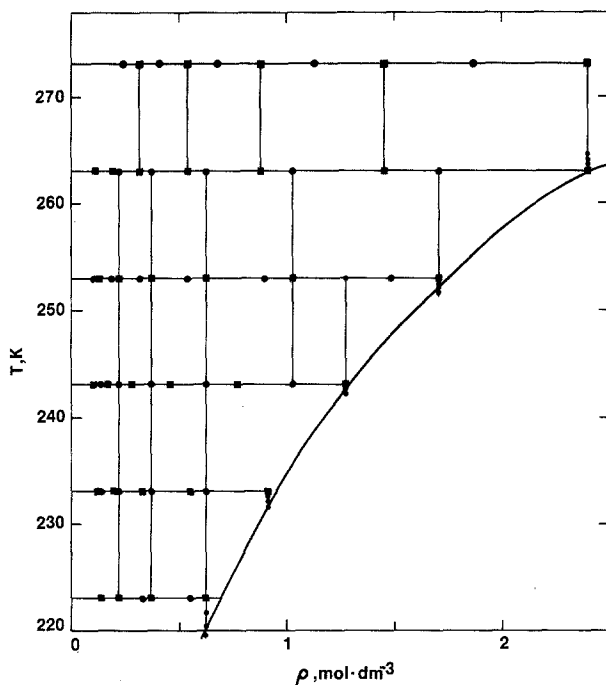

Fig. 1. Location of our experimental data points in the (T, ρ) plane. Isotherms, isochores, and the two-phase boundary are also indicated.

50 ppm C_2H_6, and 40 ppm volatiles, some of which was CH_4. Since the error induced in the second virial coefficient is of the same order as the impurity concentration [10], we felt that no further purification of the sample was necessary.

3. CELL CONSTANT AND SECOND VIRIAL OF HELIUM

The Burnett runs for helium along six isotherms are given in Table I. If we call the pressures in one run $P_0, P_1, \ldots, P_r, \ldots$, then the cell constant N is obtained by fitting the ratios P_{r-1}/P_r to a linear function of P_{r-1}:

$$P_{r-1}/P_r = N + S\,P_{r-1} \tag{1}$$

We estimate the variance of the ratio by ascribing to the pressure a variance with a constant component of $(3 \times 10^{-6}\ \text{MPa})^2$, related to the resolution of our barometer, and a proportional component of $(2 \times 10^{-5}\ P)^2$, related to the precision of our pressure gage. With absolute weights assigned accordingly, the four pressure ratios on each isotherm, which vary by no more than 0.5% over the range from 0.3 to 2 MPa, are fitted by (1) with chi-square values no higher than 0.5. An increase of the estimated constant contribution to the variance from $(3 \times 10^{-6}\ \text{MPa})^2$ to $(3 \times 10^{-5}\ \text{MPa})^2$ does not significantly

Table I. Helium Burnett runs, Cell Constant N and Second Virial Coefficient B

T (K)	273.15	263.15	253.15
P (MPa)	2.094226	2.150043	2.120296
	1.258276	1.291449	1.273415
	0.757316	0.777132	0.766221
	0.456266	0.468167	0.416559
	0.275060	0.282220	0.278232
N	1.657229	1.657207	1.657219
	$\pm 15 \times 10^{-6}$	$\pm 24 \times 10^{-6}$	$\pm 28 \times 10^{-6}$
B (cm$^3 \cdot$ mol^{-1})	11.80 ± 0.03	11.85 ± 0.06	11.87 ± 0.07
T (K)	243.15(1)	243.15(2)	233.15
P (MPa)	2.092118	2.110015	2.057672
	1.256322	1.266994	1.235437
	0.755874	0.762271	0.743248
	0.455312	0.459154	0.447675
	0.274448	0.276764	0.269844
N	1.657248	1.657234	1.657216
	$\pm 23 \times 10^{-6}$	$\pm 11 \times 10^{-6}$	$\pm 16 \times 10^{-6}$
B (cm$^3 \cdot$ mol^{-1})	11.83 ± 0.05	11.90 ± 0.03	11.97 ± 0.04

alter the results of the fit. It is seen from Table I that the intercepts of the six independent runs all overlap within their estimated standard deviations, which are of the order of a part in 10^5. In what follows, we have assumed for the cell constant N:

$$N = 1.65722 \tag{2}$$

As a byproduct of the cell constant determination, we obtain values for the second virial coefficient of helium from the slopes of the P_{r-1}/P_r versus P_{r-1} curves. It should be realized that a small part of this slope is due to the pressure dependence of the cell volumes $V(P)$, which is given by

$$\frac{V(P) - V(0)}{V(0)} = bP \tag{3}$$

with $b = 1.8 \times 10^{-5}$ per MPa for our system [10]. This pressure dependence gives rise to a pressure dependence of the cell constant:

$$N_r = N[1 - b\,(P_{r-1} - P_r)] \tag{4}$$

where N_r is defined as the value of P_{r-1}/P_r if an ideal gas were expanded in our Burnett system.

The relation between the slope S and the second virial coefficient B is then given by

$$S = (N - 1)\left[\frac{B}{RT} - b\right] \tag{5}$$

The values so obtained for B are given in Table I. All errors listed in Table I represent one standard deviation of the linear fit; Eq. (1).

Comparison of our B values with those obtained by Gammon from an analysis of his speed-of-sound data [11] reveals that our B values are systematically lower by about 0.15 cm^3 · mol^{-1}. An uncertainty in the cell deformation constant b cannot cause this much of an offset since, in (5), b contributes only 0.3% to B/RT, which corresponds with 0.03 cm^3 · mol^{-1} in B. In our fit to (4), we have neglected contributions from the third virial C. Using Gammon's C values of approximately 110 cm^3 · mol^{-1} [11], we can correct our pressure ratios for the third virial contribution. The largest change is 1 part in 10^4 in the highest ratio. This correction, however, *lowers* our B values by about 0.2–0.3 cm^3 · mol^{-1} (while it raises the cell constant 3–5 $\times$ 10^{-5}) and increases our difference with Gammon's result. The most likely explanation of this difference is a constant systematic error in our pressure.

An error of 3×10^{-5} MPa would affect principally the lowest ratio and shift it by 4 parts in 10^5 (the cell constant would experience a similar shift). This would affect the B value by roughly 1% or 0.1 cm$^3 \cdot$ mol^{-1}. An error of this order can certainly not be excluded. Since our second virials seem accurate to within 2%, our pressures are likely to be accurate to 5×10^{-5} MPa and our cell constant to 7 parts in 10^5.

4. (P, ρ, T) AND VIRIALS FOR ETHYLENE: COMPARISON

For ethylene, we took two Burnett runs along each isotherm. The highest pressure was chosen close to saturation. The data were analyzed by using the procedure of Waxman et al. [2]. Here it is assumed that no adsorption is present and that the isotherm is sufficiently defined by three virials or fewer:

$$\frac{P_r}{RT} = \rho_r (1 + B\rho_r + C\rho_r^2 + D\rho_r^3) \tag{6}$$

while

$$\frac{\rho_{r-1}}{\rho_r} = N [1 - b(P_{r-1} - P_r)] \tag{7}$$

The two initial densities $(\rho_0)_1$, $(\rho_0)_2$ and the virial coefficients B, C, and D are the unknowns to be determined by a nonlinear least-squares fit to the pressure data. We have fitted our pressure sequences with Eqs. (6) and (7), imposing the value (2) for N, using the value $R = 8.31434$ J $\cdot$ K$^{-1} \cdot$ mol^{-1}, and assigning weights as described for helium. On most isotherms, we need three virials for an adequate representation. The lowest two isotherms can be represented with only two virials. We list the densities and virials in Table II, together with the departures of the experimental points from the representation. These departures are generally less than 0.1 kPa (1 mbar). This excellent fit is, however, deceptive, as will be discussed in Section 7. Be it sufficient to point out here that (a) four or five parameters are adjusted, while the number of data points is no more than twelve in the best cases, and (b) a systematic difference from the value (2) is found if our data are fitted with N as a free parameter. In Figs. 2–4, we compare our (P, ρ, T) data with our fitted curves and with the published data of Douslin and Harrison [1], with the data of Thomas and Zander [4], and with the correlation of McCarty and Jacobsen [5]. We plot the pressure deviations, $P_{exp} - P_{calc}$, as a function of pressure along each isotherm. The slanting straight lines indicate agreement to within 1 part in 10,000 in pressure. It is clear that our agreement with the Douslin and Harrison data is better than 1 part in 5000 in the pressure. The

Table II. Ethylene Burnett Pressure P, Calculated Density ρ, and Virial Coefficients B, C, D

273.15 K			263.15 K		
P (MPa)	ρ (mol $\cdot$ dm^{-3})	$P - P_{calc}$ (kPa)	P (MPa)	ρ (mol $\cdot$ dm^{-3})	$P - P_{calc}$ (kPa)
3.53208	2.42223	−0.03	3.23689	2.42267	−0.02
2.56308	1.46161	−0.09	2.40910	1.46193	−0.02
1.71934	0.88201	−0.02	1.63456	0.88217	−0.03
1.10366	0.53225	0.04	1.05539	0.53236	0.05
0.69073	0.32117	0.01	0.66265	0.32124	0.04
			0.40937	0.19383	0.00
3.04387	1.87765	0.10	0.25050	0.11695	−0.03
2.11074	1.13297	0.00			
1.38048	0.68367	0.00	2.67780	1.71339	0.12
0.87340	0.41254	0.01	1.85882	1.03377	−0.09
0.54202	0.24893	−0.02	1.21530	0.62382	−0.05
			0.76859	0.37646	0.04
			0.47681	0.22715	0.00

$B = -167.53$ (cm$^3 \cdot$ mol^{-1})
$C = 7665$ (cm$^3 \cdot$ mol^{-1})^2
$D = 0.203 \times 10^6$ (cm$^3 \cdot$ mol^{-1})^3

$B = -180.58$ (cm$^3 \cdot$ mol^{-1})
$C = 7783$ (cm$^3 \cdot$ mol^{-1})^2
$D = 0.173 \times 10^6$ (cm$^3 \cdot$ mol^{-1})^3

253.15 K			243.15 K		
p (MPa)	ρ (mol $\cdot$ dm^{-3})	$P - P_{calc}$ (kPa)	p (MPa)	ρ (mol $\cdot$ dm^{-3})	$P - P_{calc}$ (kPa)
2.28274	1.49348	0.17	1.91698	1.27907	−0.04
1.57520	0.90105	−0.08	1.31253	0.77180	−0.07
1.02576	0.54374	−0.01	0.85038	0.46576	0.01
0.64705	0.32813	0.03	0.53476	0.28106	0.03
0.40078	0.19799	0.00	0.33062	0.16959	0.00
0.24562	0.11946	−0.02			
			1.65033	1.03455	0.10
2.48468	1.71349	−0.09	1.09899	0.62419	−0.05
1.75555	1.03405	−0.03	0.70165	0.37667	0.01
1.15748	0.62395	−0.01	0.43760	0.22730	0.01
0.73523	0.37654	0.04	0.26925	0.13714	−0.02
0.45724	0.22721	0.02			
0.28088	0.13709	−0.01			

$B = -194.71$ (cm$^3 \cdot$ mol^{-1})
$C = 7125$ (cm$^3 \cdot$ mol^{-1})^2
$D = 0.331 \times 10^6$ (cm$^3 \cdot$ mol^{-1})^3

$B = -211.57$ (cm$^3 \cdot$ mol^{-1})
$C = 7927$ (cm$^3 \cdot$ mol^{-1})^2
$D = -0.480 \times 10^6$ (cm$^3 \cdot$ mol^{-1})^3

Table II. Continued

233.15 K			223.15 K		
P (MPa)	ρ (mol · dm^{-3})	$P - P_{calc}$ (kPa)	P (MPa)	ρ (mol · dm^{-3})	$P - P_{calc}$ (kPa)
1.03969	0.62428	0.01	0.97935	0.62443	−0.01
0.66780	0.37669	−0.02	0.63369	0.37680	0.00
0.41784	0.22731	0.01	0.39801	0.22737	0.01
0.25757	0.13716	0.00	0.24586	0.13720	0.00
1.41135	0.91625	0.00	0.88545	0.55305	0.01
0.93785	0.55288	0.00	0.56784	0.33371	0.00
0.59773	0.33362	0.00	0.35491	0.20138	0.00
0.37237	0.20133	0.01			
0.22895	0.12147	−0.01			
$B = -228.78$	(cm^3 · mol^{-1})		$B = -249.17$	(cm^3 · mol^{-1})	
$C = 5044$	(cm^3 · mol^{-1})^2		$C = 2364$	(cm^3 · mol^{-1})^2	

data of Thomas and Zander show considerably more scatter and larger departures, especially at the higher pressures. At low pressures, the three data sets agree remarkably well indeed. The recent correlation by McCarty and Jacobsen [5] does not seem to do full justice to the data. Especially at low and intermediate pressures, and at the higher temperatures, the departures are systematic, approaching the 1 part in 1000 level.

The second virial data of ethylene are summarized in Table III. Again,
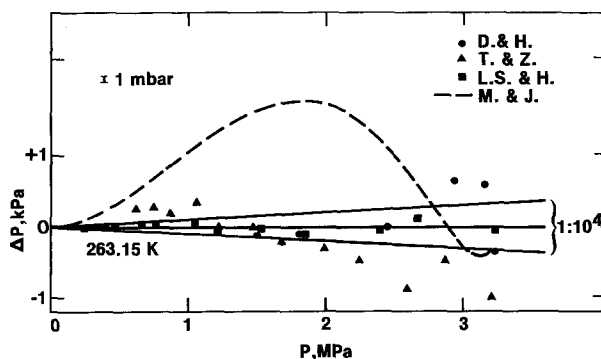
Fig. 2. Pressure difference $\Delta P \equiv P\text{-}P_{calc}$ for our data, ■; the data of [1], ●; the date of [4], ▲; and the correlation [5], dashed curve. The baseline P_{calc} is a polynomial fitted to our Burnett data (Table II).
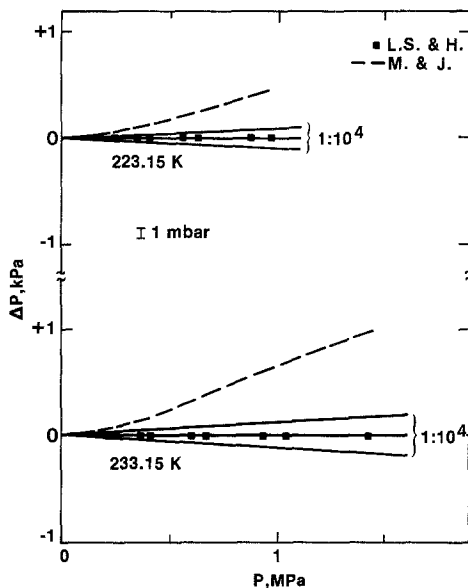
Fig. 3. Pressure difference $\Delta P \equiv P\text{-}P_{calc}$ for our data, ■; the data of [1], ●; the data of [4], ▲; and the correlation [5], dashed curve. The baseline P_{calc} is a polynomial fitted to our Burnett data (Table II).

Fig. 4. Pressure difference $\Delta P \equiv P\text{-}P_{calc}$ for our data, ■; and the correlation [5], dashed curve. The baseline P_{calc} is a polynomial fitted to our Burnett data (Table II).

Table III. Second Virial Coefficient of Ethylene, B^a

T (K)	This work	D. & H. [1]	W. & D. [3]	M. & J. [5]
273.15	−167.5	−167.6	−167.67	−164.0
263.15	−180.6	−180.9		−177.0
253.15	−194.7	−195.5		−191.5
243.15	−211.6	−212.0		−207.8
233.15	−228.8			−226.3
223.15	−249.2			−247.5

a In $cm^3 \cdot mol^{-1}$.

the agreement with Douslin and Harrison's data [1] is remarkable, within 1 $cm^3 \cdot mol^{-1}$. The data of ref. [1] do not extend to pressures below 1 MPa; the authors must be commended for the excellence of their data and the reliability of their extrapolation technique!

The third virial data are shown in Table IV. Again, the agreement with Douslin and Harrison's data is striking. There may be a systematic change in C between 253.15 and 243.15 K because of the changeover from a cubic to a quadratic equation. Our agreement with the virial data of Waxman and Davis [3] at 273.15 K leaves nothing more to be desired.

5. ISOCHORIC COUPLING

The results of coupling our Burnett isotherms isochorically are summarized in Table V. We will discuss one example in detail: the others will be self-explanatory. Consider the coupling of the 263.15 K isotherm to the one at 273.15 K. The 263.15 K run was started by filling the apparatus to 3.53197 MPa at 273.15 K. This pressure is extremely close to the point 3.53208 MPa

Table IV. Third Virial Coefficient of Ethylene, C^a

T (K)	This work	D. & H. [1]	W. & D. [3]
273.15	7.67×10^3 (cubic)	7.90×10^3	7.775×10^3
263.15	7.78×10^3 (cubic)	8.18×10^3	
253.15	7.13×10^3 (cubic)	8.09×10^3	
243.15	7.93×10^3 (cubic)	7.80×10^3	
233.15	5.04×10^3 (quadr.)		
223.15	2.36×10^3 (quadr.)		

a In $(cm^3 \cdot mol^{-1})^2$.

Table V. Isochoric Coupling

P (MPa)	ρ (mol · dm^{-3}) (Burnett isotherm)	P (MPa)	ρ (mol · dm^{-3}) (Burnett isotherm)	ρ (mol · dm^{-3}) isochore	$\Delta\rho/\rho$ (%)
263.15 K		to		273.15 K	
3.23689	2.42267	3.53197	2.42210	2.42158	0.021
2.40910	1.46193		1.46151	1.46127	0.016
1.63456	0.88217		0.88197	0.88177	0.023
1.05539	0.53236		0.53222	0.53212	0.019
0.66265	0.32124		0.32115	0.32110	0.02
253.15 K		to		263.15 K	
2.48468	1.71349	2.67770	1.71330	1.71272	0.034
1.75555	1.03405		1.03372	1.03358	0.014
1.15748	0.62395		0.62379	0.62367	0.019
0.73523	0.37654		0.37644	0.37637	0.02
0.45724	0.22721		0.22714	0.22710	0.02
243.15 K		to		253.15 K	
1.65033	1.03455	1.75552	1.03403	1.03408	0.005 −
1.09899	0.62419		0.62394	0.62391	0.005
0.70165	0.37667		0.37653	0.37650	0.008
0.43760	0.22730		0.22720	0.22720	0.000
0.26925	0.13714		0.13709	0.13708	0.007
233.15 K		to		243.15 K	
1.03969	0.62428	1.09892	0.62415	0.62400	0.024
0.66780	0.37669		0.37665	0.37652	0.035
0.41784	0.22731		0.22728	0.22721	0.03
0.25757	0.13716		0.13713	0.13710	0.02
223.15 K		to		233.15 K	
0.97935	0.62443	1.03969	0.62428	0.62415	0.021
0.63369	0.37680		0.37669	0.37663	0.02
0.39801	0.22737		0.22731	0.22727	0.02
0.24586	0.13720		0.13716	0.13714	0.01

on this isotherm, obtained in a previous Burnett run that was completely analyzed; $\rho = 2.42223$ mol · dm^{-3} (Table II). A small adjustment therefore gives the density of the point at 3.53197 MPa, namely, 2.42210 mol · dm^{-3}. All subsequent densities, 1.46151 mol · dm^{-3}, etc. can likewise be predicted from the 273.15 K Burnett isotherm. Now the system is cooled to 263.15 K and a Burnett run is done. This run and its companion at 263.15 K can be fully analyzed to obtain the densities in the second column of Table V, which are simply copied from Table II. If we accept these density values, we can reconstruct the densities at 273.15 K by correcting them for the thermal
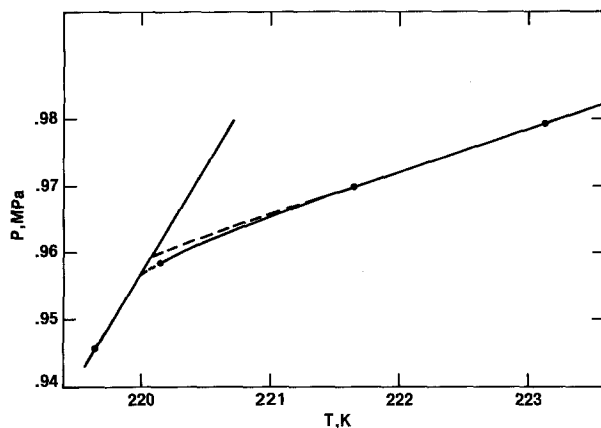
Fig. 5.   Intercept of the 0.624 mol·dm⁻³ isochore with the vapor
pressure curve.

expansion of the stainless steel vessels, 45×10^{-6} per K [10]. This yields the
densities labeled "isochore" under 273.15 K. It is clear that the isochore
densities are slightly less than the Burnett densities. The difference $\Delta\rho/\rho$
persists at all temperatures and is usually of the order of 0.015%. This
difference may be due to gas adsorbed at the lower temperature and freed at
the higher one. The "isochore" density does not account for this extra
amount. The question of whether, and how much, error is introduced into our
Burnett (P, ρ, T) data by this effect will be discussed in Section 7.
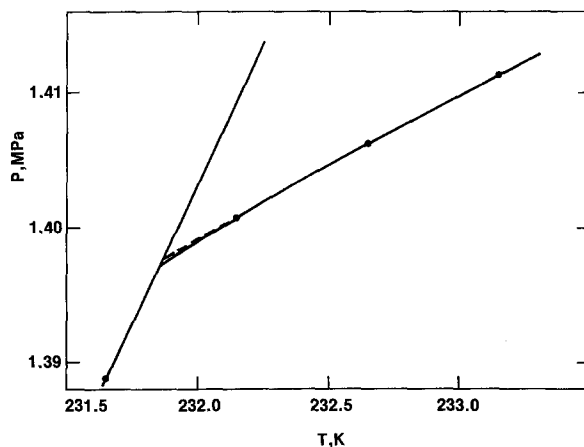
Fig. 6.   Intercept of the 0.916 mol·dm⁻³ isochore with the
vapor pressure curve.
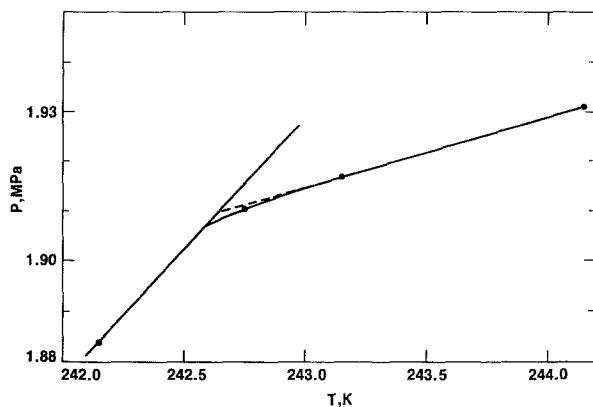
Fig. 7. Intercept of the 1.28 mol·dm⁻³ isochore with the vapor
pressure curve.

6. THE VAPOR BOUNDARY

In Figs. 5–9, we show the finely spaced (P, T) data obtained on
isochores entering the two-phase region. The data are summarized in Table
VI. Densities can be assigned to these isochores from points they contain at
temperatures where Burnett runs have been taken. In general, more than one
point is available. Their densities are underlined in Table VI. Again, we
observe the fact found in the previous section: the lower the temperature of
the anchor point, the lower the value of the density predicted at a given
temperature, which may indicate that molecules are removed from the bulk
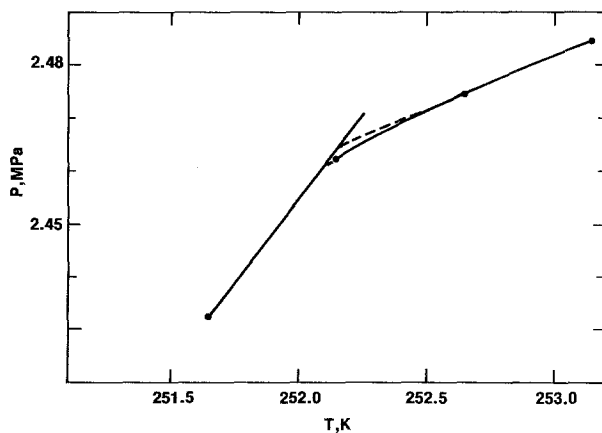
Fig. 8. Intercept of the 1.71 mol·dm⁻³ isochore with the vapor
pressure curve.
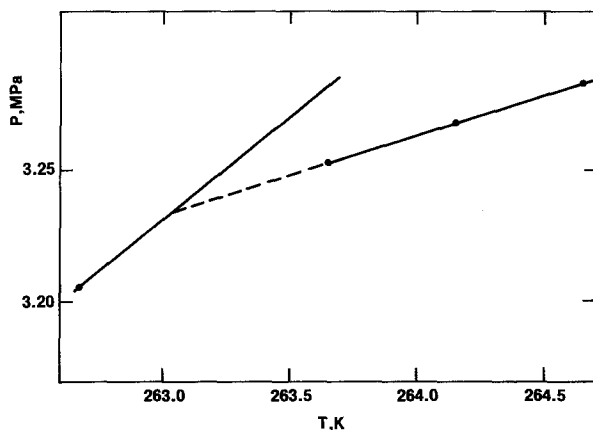
Fig. 9. Intercept of the 2.42 mol·dm^{-3} isochore with the vapor pressure curve.

by adsorption. Close to the phase boundary, these effects seem exaggerated and amount to several parts in 10,000 in some cases. Thus one source of error in assigning a density to the isochoric intercept is the variation in density assignment to the isochore arising from the use of different anchor points.

A second source of error is the definition of the vapor pressure curve. We have previously measured this curve at fill densities near critical and using the same sample source, but with volatiles removed [9]. It is clear from Table VI that our present vapor pressures are a few 0.1 kPa (a few mbar) below those obtained before. A glance at Figs. 5–9, however, convinces one that this indeterminacy is minute compared to the most glaring source of error: the strong curvature of the isochores as the vapor boundary is approached. In our opinion, this strong curvature is an artifact induced by surface effects. In Table VII, we mark the temperature of the isochoric intercept for the real curved isochore, and for a straight extrapolation (Figs. 5–9). For the density assignment, we prefer the value obtained from the Burnett run closest to the intercept. Douslin and Harrison [1] obtained their vapor densities from intercepts along isotherms, and represented these densities closely by a three-term equation in temperature. We have used their equation to predict our densities at our intercept temperatures; see the last column of Table VII. Values in parentheses are outside the range of applicability of the equation. If we calculate saturation vapor densities by "straight" extrapolations of the isochores, the results agree favorably with saturation densities calculated from the vapor density equation of Douslin and Harrison. If the intercept is taken on the actual curved isochore, the departures between the vapor density values can be quite large, up to 1 part in 600 at 252 K. In our view, at the

Table VI. Ethylene Isochoric Intercepts with Phase Boundary

T (K)	P (MPa)	ρ (mol · dm^{-3})		P_{vap} [9] (MPa)
273.15	3.53195	2.42207		
264.65	3.28264	2.42301		
264.15	3.26762	2.42306		
263.65	3.25252	2.42312		
262.675	3.20581			3.20598
263.15	2.67770	1.71329		
253.15	2.48468	1.71407	1.71349	
252.65	2.47462	1.71411	1.71353	
252.15	2.46247	1.71414	1.71357	
251.65	2.43238			2.43253
253.15	2.05438	1.27860	1.27850	
244.15	1.93133	1.27911	1.27902	
243.15	1.91699	1.27917	1.27908	
242.75	1.91034	1.27919	1.27910	
242.15	1.88357			1.88385
243.15	1.50464	0.91606		
233.15	1.41135	0.91647	0.91625	
232.65	1.40631	0.91649	0.91627	
232.15	1.40079	0.91651	0.91629	
231.65	1.38781			1.38822
243.15	1.09892			
233.15	1.03969	0.62428		
223.15	0.97935	0.62456	0.62443	
221.65	0.96994	0.62460	0.62447	
220.15	0.95855	0.62464	0.62451	

approach to the two-phase boundary, a liquid film is formed on some or all surfaces exposed to the vapor; this process reduces the density of the vapor by an amount that appears to be of the order of one part in 10^3. Since the geometric area exposed to the vapor is of the order of 70 cm^2, a monolayer of liquid would contain no more than 3×10^{-8} mol. Near saturation, our system contains 2×10^{-2} mol. For a one-part-in-10^3 effect on the vapor density, 1000 monolayers, or a film close to a micron thick, would have to have been present. More likely, precondensation took place in the narrow capillaries or between the closely-spaced surfaces of the transducer.

7. ACCURACY

We first discuss the uncertainty introduced in the density by the uncertainties of the experimental parameters and by the Burnett data

Table VII. Vapor Phase Boundary

Temperature of intercept, T (K)		Isochore density, ρ (mol $\cdot$ dm^{-3})	Predicted density, eqn. D. & H. [1], ρ (mol $\cdot$ dm^{-3})
Actual	263.04	2.4231	2.4241
"Straight"			
Actual	252.09	1.7136	1.7099
"Straight"	252.15		1.7131
Actual	242.58	1.2791	1.2759
"Straight"	242.63		1.2778
Actual	231.85	0.9163	(0.9160)
"Straight"	231.86		(0.9163)
Actual	219.99	0.6245	
"Straight"	220.08		

analysis. Next the evidence for adsorption is discussed, and the uncertainty introduced by it in the density is considered.

In the Burnett method, only pressure and temperature are measured directly. Our temperature control and measurement are accurate to 1 mK or better; negligible density error results from this uncertainty. The absolute accuracy of our pressure gage was estimated to be 1 part in 20,000 [8]; a proportional error in the pressure will generate a density error of similar size, 5 parts in 10^5 in this case. As explained in Section 3, there is evidence to believe that the absolute error in the pressure is determined by the limited accuracy of the barometer and may be of the order of 3×10^{-5} MPa; this limits the accuracy of the cell constant, as determined by helium expansion, to 7×10^{-5} or 4 parts in 10^5. In Burnett runs with five expansions, one expects an error of at most 2 parts in 10^4 from this uncertainty. Uncertainties in the thermal expansion coefficient do not affect the densities obtained from Burnett analysis; they could, however, affect the deficit of 0.015% in density that we detected between successive isotherms. We used the value 45×10^{-6} per K for the volume expansion of our vessels and corroborated this value to 10% uncertainty by coupling our helium isotherms along one isochore [10]. This 10% uncertainty will cause an uncertainty of 30% in the reported density deficit.

For the pressure expansion of the vessels, we used a value of 1.8×10^{-5}

per MPa, estimated for infinitely long stainless steel cylinders. Although this value is not precise, the pressure expansion of our cylinders in this low-pressure region is small enough that even a 20% error in the expansion coefficient causes less than 1 part in 10^5 error in the sample volume.

Additional uncertainty in the density is introduced by the data analysis. The high nonideality of the gas requires the inclusion of several virials in the data analysis even though the pressure range was quite small. Thus the number of adjustable parameters was high, 4 or 5, while the number of data points was small, 12 or less. This led to very close fits with high correlation between the parameters, while there was little flexibility left for testing range dependence, dependence on the number of terms in the virial expansion, etc. We did analyze the isotherms, omitting the point near saturation, and also, in limited pressure ranges, with two rather than three virials. In general, and especially at the lowest temperatures, the density values obtained at each (P, T) point in these various ways agreed to 1 part in 10^4 or better. Only at the 263.15 K isotherm did the density drop by as much as 1 part in 4000 at some points when the pressure nearest saturation was omitted. The second virial values varied by about 0.5 cm^3 · mol^{-1} when the fitting procedure was modified in the way described. Thus it seems safe to assume that the combined uncertainties in the measurement of the physical parameters, in the determination of the cell constant, in the data analysis, and due to the presence of precondensation cause uncertainties in the density that will not exceed 1 part in 3000, and errors in the second virial of about 0.5 cm^3 · mol^{-1}.

This leaves us with the discussion of the effects of adsorption. There are two reasons why we suspect the presence of nonnegligible adsorption in our work. As discussed in Section 5, we have found a nontrivial decrease of about 0.015% in density for a 10 K decrease in temperature if the Burnett densities are accepted as correct and the isotherms are coupled isochorically. In addition, we have found that if the cell constant N is treated as a free parameter in the fit, it is generally higher than the value obtained from helium expansion, which is a well-known warning signal for the presence of adsorption [12]. As to the last point, our free-N results have the following features. From 273.15 to 243.15 K, inclusive, the free-N values for the full data range, with the use of three virials, are from 2.6 to 3.5 parts in 10^4 above the helium N value; this offset exceeds the standard deviation of the free-N result by a factor 4–6. If two virials are used in more limited pressure ranges, the free-N value drops, but not enough to agree with the helium N value. This result is somewhat inconclusive due to the low number of degrees of freedom (typically 1!). Omission of the pressure point near saturation leads to a small decrease in the free-N value. At the low temperatures, 233.15 and 223.15 K, where only two virials are required, the free-N result agrees with the fixed-N

value to within a standard deviation of the free-N result. Thus at the higher temperatures, there is a high value of the free N, which, in small part, is due to the high nonideality of the isotherm, and, for the main part, could be due to adsorption. At the lowest isotherms, surprisingly, this increase in N is not seen.

The following facts about our system are relevant in a discussion about adsorption. Our principal vessel plus transducer have a volume of $\sim$10 cm^3 and a surface area of $\sim$70 cm^2. The two expansion vessels combined have a volume of $\sim$5 cm^3 and a surface area of $\sim$15 cm^2. The internal surfaces of the vessels are finished to 4×10^{-5} mm and gold-plated. Vessels, transducers, valves, and capillaries are made of stainless steel. The principal vessel and appendages contain no nonmetallic part. The expansion volume is exposed to two Teflon valve packings of 6 mm diameter, 3 mm thickness, strongly compressed between two washers.

Application of the BET equation for multilayer adsorption [13] shows that a monolayer is present even at our lowest pressures, while two or three layers are present through most of the range. If we assume that a monolayer is 4×10^{-8} cm thick and has a density equal to that of the liquid, we estimate that at intermediate pressures, a fraction of roughly 2×10^{-5} of the molecules are adsorbed, which is negligible. Moreover, in a 10 K interval along a path of a constant number of molecules, an additional fraction of 5×10^{-6} would be adsorbed or desorbed. The observed deficit is a factor 30 higher. We consider it unlikely that the surface area would exceed the geometric area by that large a factor and therefore have to reject adsorption on the walls of the principal volume as an explanation for our observations of surface effects.

Adsorption of a pressure-independent amount of gas in the principal vessel is of no concern in the first place; in the expansion volume, it is a cause of concern since the adsorbed layer is removed at each evacuation: an apparent increase in the expansion volume and therefore in the cell constant is the result. Again, however, a simple order-of-magnitude estimate based on the BET equation applied to the geometric surface area leads to a shift in N by roughly a factor 30 smaller than observed.

It is possible that ethylene enters into the pores or diffuses into the bulk of the Teflon packings. The pore hypothesis will only give rise to a shift in N if we assume that the ethylene density in the pores is higher than in the bulk, since the helium N value includes the pore volume. If ethylene would, at all pressures, be present in the pores as a liquid, a pore volume of less than 0.1% of the packing volume would explain the observed shift in N. The diffusion hypothesis would lead one to expect slow equilibration, drift, hysteresis, and irreproducibility of pressure measurements, effects that were never found in our experiment.

The porosity hypothesis leads to the worst-possible scenario. If we

hypothesize, as a model, that a constant amount of gas is present in, and extracted from, the pores on evacuation along a given isotherm, then we find that a Burnett analysis ignoring this effect will yield densities that are off by as much as a part in 2000 at the high pressures (if N_{free} and N_{fixed} differ by 4 parts in 10^4). If the amount decreases with temperature, as is reasonable to assume, this could explain the observed isochoric deficits. The porosity hypothesis does not explain why no shifts in N were observed at the lowest temperatures.

The best-possible scenario results from the hypothesis that the Burnett densities are essentially correct, that the free-N shifts are artifacts due to the high nonideality of the gas, and that the isochoric density deficits are due to either the presence of an unknown (but harmless) adsorber in the principal vessel, to an overestimate of the expansion coefficient, or to a peculiarity of the transducer volume.

Since we do not have the information needed to decide between these scenarios, we have to admit that the total error in our higher densities could be high as the sum of 1 part in 3000 and 1 part in 2000, that is, 8 parts in 10,000. Our fine agreement with the results of [1] gives us hope that the estimate of 1 part in 3000 is closer to the truth.

ACKNOWLEDGMENTS

REFERENCES

1. D. R. Douslin and R. H. Harrison, *J. Chem. Thermodyn.* **8**:301 (1976).
2. M. Waxman, J. R. Hastings, and W. T. Chen, in *Proc. 5th Symp. Thermophys. Prop.*, C. F. Bonilla, ed. (ASME, New York, 1970), p. 248.

---

[3]In order to describe materials and experimental procedures adequately, it is occasionally necessary to identify commercial products by manufacturer's name or label. In no instance does such identification imply endorsement by the National Bureau of Standards, nor does it imply that the particular product or equipment is necessarily the best available for the purpose.

M. Waxman, H. A. Davis, and J. R. Hastings, *Proc. 6th Symp. Thermophys. Prop.,* P. E. Liley, ed. (ASME, New York, 1973), p. 245.

3. M. Waxman and H. A. Davis, *Adv. Chem.* **182**(16):285 (A.C.S. Washington, D.C., 1979).
4. W. Thomas and M. Zander, *Int. J. Thermophys.* **1**:383 (1980).
5. R. D. McCarty and R. T. Jacobsen, NBS Tech. Note (in press).
6. G. A. Pope, P. S. Chappelear, and R. Kobayashi, *Physica* **57**:127 (1972).
7. K. R. Hall and P. T. Eubank, *Physica* **61**:346 (1972).
8. J. M. H. Levelt Sengers and W. T. Chen, *J. Chem. Phys.* **56**:595 (1972).
9. J. R. Hastings and J. M. H. Levelt Sengers, *Proc. 7th Symp. Thermophys. Prop.,* A. Cezairliyan, ed. (ASME, New York, 1977), p. 794.
10. J. R. Hastings, J. M. H. Levelt Sengers, and F. W. Balfour, *J. Chem. Thermodyn.,* **12**:1009 (1980).
11. B. E. Gammon, *J. Chem. Phys.* **64**:2556 (1976).
12. P. T. Eubank and W. J. Kerns, *A.I.Ch.E. J.* **19**:711 (1973).
13. S. Brunauer, *Physical Adsorption* (Princeton University Press, Princeton, N.J., 1943).